Highlights of Spanish Astrophysics XI, Proceedings of the XV Scientific Meeting of the Spanish Astronomical Society held on September 4–9, 2022, in La Laguna, Spain. M. Manteiga, L. Bellot, P. Benavidez, A. de Lorenzo-Cáceres, M. A. Fuente, M. J. Martínez, M. Vázquez- Acosta, C. Dafonte (eds.), 2023

Determining the orbital parameters of binary systems with an AGB primary. The case of the R Aqr symbiotic system.

Alcolea, J.[1], Mikołajewska, J.[2], Gómez-Garrido, M.[1], Bujarrabal, V.[1], Iłkiewicz, K.[2], Castro-Carrizo, A.[3], Desmurs, J.-F.[1], Santander-García, M.[1], and Bachiller, R.[1]

[1] Observatorio Astronómico Nacional (IGN, Spain)
[2] Centrum Astronomiczne im. Mikołaja Kopernika (PAN, Poland)
[3] Institute de Radioastronomie Millimétrique (France)

Abstract

Binary stars including an AGB star hold the clues for understanding important phenomena in stellar evolution, such as common-envelope events, the formation of SN-Ia, and the origin of aspherical pPNe/PNe. Hydro-dynamical codes simulating the companion's influence on the primary mass loss exist, but we still lack information on the orbital parameters of systems where these models can be tested. The best case where this can be pursued is R Aqr. Here, we present the results of the first-ever determination of the whole set of orbital parameters of the system purely based on observational data. The results agree very well with the observational characteristics of the nebula around the system. Reasonable values for the stellar masses agree with distances from period- and diameter-luminosity relationships for Mira variables, but not with those from VLBI observations of SiO masers or GAIA.

1 AGB binaries and the case of R Aqr

Binary systems are interesting astrophysical laboratories as they are responsible for several extreme physical phenomena. In addition, when the system is spatially resolved and we know the velocity curve for at least one star, we can derive the (otherwise elusive) individual masses of the member stars. Binary stars including an Asymptotic Giant Branch (AGB) primary are particularly interesting since the presence of a compact companion can induce a mass transfer process that can severely affect the evolution of both members. AGB stars lose mass at such high rates (up to 10^{-5} $M_\odot\,yr^{-1}$) that this process is ultimately responsible for the evolution of the star into a white dwarf (WD). This wind forms a circumstellar envelope (CSE), rich in molecular gas and dust particles, around the AGB star, which will turn into a planetary nebula (PN) in the forthcoming post-AGB phases. The standard theory predicts that AGB CSEs should be roughly spherical. However, this may not be the case for AGB

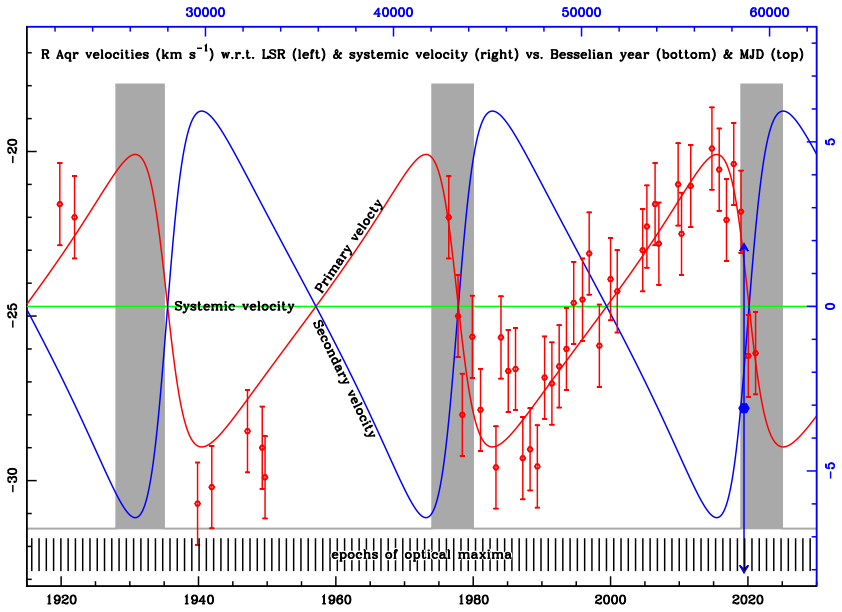

Figure 1: The updated velocity curve of the primary, the Mira variable R Aqr-A, based on the data presented by [7], but including new values from SiO maser observations up to mid-2021. Data are averaged for each pulsation period (black lines at the bottom show the dates for R Aqr optical maxima according to AAVSO). Red dots show the observed values (with $\pm 1.25\,\mathrm{km\,s^{-1}}$ error bars), while the red and green lines show the fitting to the data and the systemic velocity of the centre of masses. The blue line displays the prediction for the companion velocity for a mass ratio of 1.4. The blue dot (and error bar) shows de velocity derived for the companion R Aqr-B for 2019.4 from the H30α line. The dark areas mark the occurrence of eclipses in the system.

binaries, where the presence of the companion breaks the spherical symmetry: the launching of bipolar jets by these companions (powered by mass accretion from the primary) is the most plausible explanation for the formation of axis-symmetric PNe via their interaction with the AGB wind (see e.g. [5]). This hypothesis is supported by the presence of spiral density waves in the CSEs of many AGBs [6], which can be easily explained as a result of the gravitational pull of the companion on the AGB star, and the focusing of the mass-loss on the orbital plane. These spiral-like features are not only seen in AGB CSEs but also in some PNe (e.g. NGC 7027, NGC 3132), and the transition objects in between them (e.g. the pre-PNe CRL 2688), strengthen the evolutive relationship between these three kinds of sources.

Although hydrodynamical models for binary systems with an AGB mass-losing primary reproduce the observations (e.g. [11]), an independent measurement of the orbital parameters is mandatory to establish the connection between the companions and the arising of these spiral density waves, which is the best support for the binary/aspherical-PNe link hypothesis. So far, there is only one case in which the spiral imprint is detected and we can find about the orbital parameters of the system: the symbiotic star R Aqr.

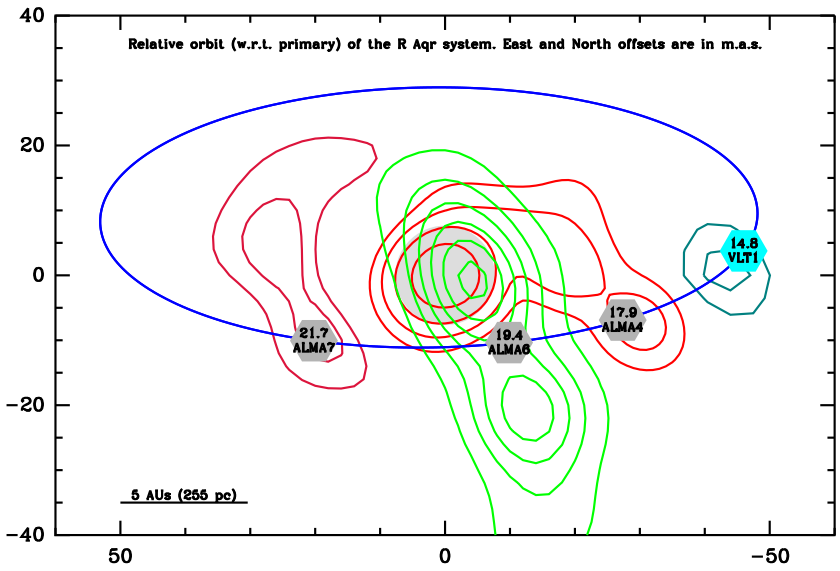

Figure 2: Relative positions of the WD secondary w.r.t. the Mira primary for the four observed epochs. We include the VLT results by [15] (2014.8, teal green contours), and ALMA 0.8 mm continuum by [3] (2017.9 red contours). For 2019.4, the secondary is assumed to be at the centre of the jet seen in H30α (green contours). For 2021.7, we assume that the secondary is at the southernmost end of the 0.8 mm continuum after removing the contribution of the primary (dark red contours). Both 2019.4 and 2021.7 positions are from unpublished ALMA observations. The position of the primary is always at the origin of the coordinates. East and North offsets are in mas. The grey disk at the centre shows the size of the primary ($\sim$17 mas). The relative orbit in the plane of the sky resulting from the fitting is shown by the blue ellipse: the system rotates clockwise. Predictions for the epochs of the observations are marked by hexagons. Scale in AUs for a distance of 255 pc is also indicated.

R Aqr is a symbiotic system consisting of a primary AGB star (R Aqr-A) and a WD secondary (R Aqr-B). Located 220–385 pc away [14, 2], it is one of the closest interacting binaries. As a result of mass accretion, the companion launches a bipolar precessing jet that illuminates an arc-minute-wide point-symmetric nebula [12] (supporting the link between aspherical PNe and binary stars). ALMA CO mapping has revealed the strong shaping of the CSE by the companion, with the detection of a two-arm spiral in molecular gas [3, 4]. In addition to the composite stellar spectrum [13], the occurrence of eclipses [16] and the regular variations of the velocity of the primary [9] support the binary nature of the system, also suggesting an orbital period of $\sim$40–44 a. Based on these results [10, 7] performed the first attempts to derive the orbital parameters of the system. However, these calculations were based on a wrong identification of the secondary [10] and some assumptions on the orientation of the orbit; it was not till 2014–17 that the two components were finally resolved through VLT [15] and Cycle-4 ALMA observations [3]. In this contribution, we present the first determination of the full set of orbital parameters for the R Aqr-AB system purely based on observational data, which include an updated dataset for the radial velocity of the primary,

and additional Cycle-6 and -7 ALMA observations of the relative position of the two stars.

2 The new/updated observational data and their fitting

One of the problems inherent to the determination of the orbital parameters in systems involving a Mira star is that the expected variations in the radial velocity are smaller than those due to its regular pulsations [9]. This problem can be partially overcome by using radial velocities derived from the SiO maser emission, which is so common in O-rich Mira stars. Due to pumping constraints, these emissions come from regions at a few stellar radii, where the pulsation effects are not so strong. In addition, maser amplification favours the detection of regions close to the plane of the sky [1], where Doppler shifts due to radial movements are largely suppressed. In this work, we have used the radial velocity curve compiled by [7] but updated with newer SiO observations up to May 2021, including those from the new Yebes monitoring of SiO masers in evolved stars. To further minimize the possible effects of the stellar pulsation, velocity data have been averaged for each pulsation period (following AAVSO database results for optical variability period and epochs of maxima). After this binning, we adopted the midpoint between the maximum and minimum velocity observed in SiO maser emission as the radial velocity for the primary for the corresponding pulsation period. The results are shown in Fig. 1.

For the first time, we have combined the velocity curve of the primary, with data for the relative position between the two components for several epochs. In addition to the published data by [15, 3], we have also included new Cycle-6 and -7 ALMA maps for epochs 2019.4 and 2021.7 respectively, both with spatial resolutions of about 20 mas (see Fig. 2). In 2019.4, the system was observed very closely to its inferior conjunction: we could not separate the 1.3 mm continuum emission of the secondary from the much stronger primary (as we did for the 2017.9 observation [3]). However, we have identified the position of the secondary as the mid-point of the two-sided jet structure seen in H30α (see the contribution by Gomez-Garrido *et al.* in these proceedings). In 2021.7, due to the larger separation of the stars, the secondary has been identified at the base of the elongated structure (the jet) seen in the 0.8 mm continuum image after the removal of the primary's contribution.

The combined velocity and relative position data are fitted for the determination of the orbital parameters of the system. We have used the code BINARY by Donald H. Gudehus [8]. The resulting set of parameters is shown in Table 1. The predictions for the primary's velocity curve and relative position of the stars based on these orbital parameters are also shown in Figs.1 and 2. A short movie of the configuration of the system in the orbital plane can be seen in this YouTube link. For a distance of 255 pc (see next section), the separation between the stars varies between 8 and 21 AUs, the periastron occurring very close to the inferior conjunction. The inclination of the orbit agrees very well with that of the ring seen in the optical nebula at much larger scales [12], supporting our results and that the ring is also due to interactions in the system.

Table 1: Campbell's elements for the R Aqr system derived from the fitting

Parameter name	Symbol	Value	Error	Units
Revolution period	P	42.4	$\pm$0.2	a
Periastron epoch	T	2019.9	$\pm$0.1	BSY
Eccentricity	e	0.45	$\pm$0.01	
Position angle of ascending node	Ω	91.4	$\pm$0.7	deg.
Inclination	i	110.7	$\pm$1.0	deg.
Angle of line of nodes to periastron	ω	84.8	$\pm$2.5	deg.
Major semi-axis	a	57	$\pm$8	mas

3 Implications on the distance to R Aqr

The fitting of the new data provides values for all the orbital parameters without requiring any assumptions. However, we need the distance to the system to estimate the masses. Inversely, if we can provide some guesses on the masses of the stars, we can determine the distance. These dependencies are very steep as the system's total mass is proportional to the distance to the third power. A plot of the system's total mass, as well as for individual stars, as a function of the assumed value for the distance to R Aqr is displayed in Fig 3. Other properties of the Mira primary, such as elemental/isotopic abundances and the pulsation period suggest a mass of $\sim 1\,M_\odot$, in agreement with the values obtained from the orbital parameters for the distances based on general properties of Mira variables (period-luminosity and diameter-luminosity relationships). On the contrary, for the distances derived from trigonometric parallaxes by VLBI observations of SiO masers and GAIA, we obtain masses for the Mira that are either too low or too high, respectively. We, therefore, conclude that, unless the presence of the companion strongly modifies the basic stellar properties of the primary, the most likely distance to the system is 255 pc, resulting in a total mass of $2.7\pm0.1\,M_\odot$, a mass ratio of 1.4, and individual masses of 1.0 ± 0.2 and 0.7 ± 0.2 $M_\odot$ for the Mira and WD, respectively. We also conclude that the most likely explanation for the wrong distance estimation by the parallax methods is the size of the primary and the orbital motion around the barycentre, which are both larger than the parallaxes determined.

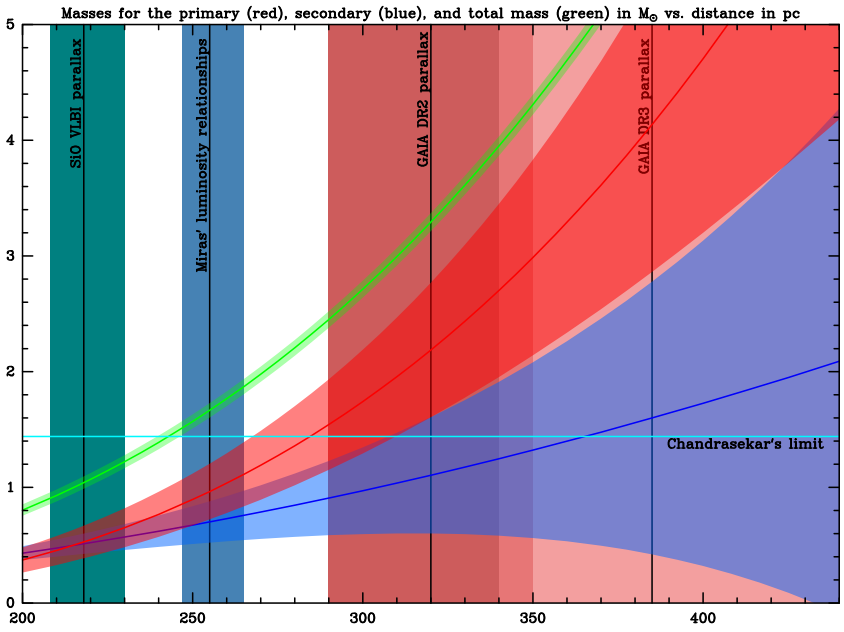

Figure 3: Masses and confidence intervals (in $M_{\odot}$) for the primary (red), secondary (blue), and total mass (green) as a function of the distance to R Aqr (in pc). The vertical black lines and coloured areas show the values and confidence intervals for the distance estimated using different methods. In teal green, the distance by VLBI parallax of SiO masers by [14]; in steel blue, that from pulsation-period and diameter versus luminosity relationships for Mira variables; and in dark/light red, values from GAIA DR2/DR3. Both VLBI and GAIA distances result in masses either too low or too high. The most reasonable values are those given by the Miras' luminosity relationships; see Sect. 3.

Acknowledgments

Authors acknowledge the support of the Spanish Ministry of Science and Innovation through the AEI research grant PID2019-105203GB-C21 (EVENTs / Nebulae Web project).

References

[1] Alcolea, J., 2004, 7th EVN Symp., 169A

[2] Bailer-Jones, C.A.L., Rybizki, J., Fouesneau, M., *et al.*, 2021, AJ 161, 147B

[3] Bujarrabal, V., Alcolea, J., Mikołajewska, J., *et al.*, 2018, A&A 616L, 3B

[4] Bujarrabal, V., Agúndez, M., Gómez-Garrido, M., *et al.*, 2021, A&A 651A, 4B

[5] De Marco, O., Akashi, M., Akras, S., *et al.*, 2022, NatAs 6, 1421D

[6] Decin, L., Montargès, M., Richards, A.M.S., *et al.*, 2020, Sci 369, 1497D

[7] Gromadzki, M., & Mikołajewska, J., 2009, A&A 495A, 931G

[8] Gudehus, D.H., 2001, BAAS 33, 850G

[9] Hinkle, K.H., Wilson, T.D., Scharlach, W.W.G, & Fekel, F.C., 1989, AJ 98, 182H

[10] Hollis, J.M., Pedelty, J.A., & Lyon, R.G., 1997, ApJ 482L, 85H

[11] Kim, H. & Taam, R.E., 2012, ApJ 759L, 22K

[12] Liimets, T., Corradi, R.L.M., Jones, D., *et al.*, 2018, A&A 612A, 118L

[13] Merrill, P.W., 1935, ApJ, 81, 312M

[14] Min, C., Matsumoto, N., Kim, M.K., *et al.*, 2014, PASJ 66, 38M

[15] Schmid, H.M., Bazzon, A., Milli, J, *et al.*, 2017, A&A 602A, 53S

[16] Willson, L.A., Garnavich, P., & Mattei, J.A. 1981, IBVS 1961, 1W